

Biermann battery effects on the turbulent dynamo in a colliding plasma jets produced by high-power lasers

Chang-Mo Ryu^{a,*}, Huynh Cong Tuan^a, Chul Min Kim^{a,b,*}

^aCenter for Relativistic Laser Science, Institute for Basic Science, Gwangju 61005, Korea

^bAdvanced Photonics Research Institute, Gwangju Institute of Science and Technology, Gwangju 61005, Korea

Abstract

The implication of the Biermann battery (BB) on turbulent magnetic field amplification in colliding plasma jets produced by high-power lasers is studied by using the FLASH code. It is found that the BB can play a significant role in turbulent field amplification. The small scale fluid structures introduced by turbulence can allow the BB to effectively amplify the magnetic field. When the flow is perpendicular to the magnetic field, the magnetic field amplification is shown to be greater than the case where the flow is parallel.

Keywords: Plasmas, Laser, Biermann battery, Turbulence dynamo, Laboratory astrophysics

1. Introduction

One of the fundamental issues in astrophysical plasmas is the magnetic field generation and amplification, which is often dubbed as the dynamo mechanism [1, 2, 3]. There is rich literature on the dynamo mechanism. Several mechanisms such as turbulence [3], Biermann battery (BB) [4, 5], Weibel instability [6, 7], and stochasticity [8] have been proposed for the dynamo mechanism. Medvedev et al. showed by using a particle-in-cell (PIC) simulation that the cosmic magnetic field can be generated by the Weibel instability, which is amplified by turbulence in a collisionless shock for Mach number $M \sim 6$ [9]. Schoeffer et al. studied the transition between the Weibel and Biermann regimes by using a PIC simulation [10]. With the advent of high-power lasers, it has now become possible to study such magnetic generation and amplification mechanisms in the laboratory. Kugland et al. reported a self-organized electromagnetic field in a laser-produced supersonic counter-streaming plasmas [11], and Huntington et al. reported an observation of the Weibel-filamentation to generate magnetic field in counter streaming plasma flows [12]. Recently, Tzeferacos et al. [13] have demonstrated turbulence amplification of the magnetic field in laser-produced plasmas which could be relevant to astrophysical situations such as interstellar media, galactic disks, and plasma jets in gamma ray bursts.

In this paper, we present our simulation study of magnetic field amplification in colliding plasma jets. To understand the effects of the BB on the turbulence dynamo, we applied uniform seed magnetic fields parallel and perpendicular to the flow direction. Our simulation shows

that the Kelvin–Helmholtz (KH) instability is initially excited, which quickly develops into turbulence. The BB effects are found to be important for turbulent magnetic amplification. The BB effects are more conspicuous when the magnetic field is in the perpendicular direction.

This paper is organized as follows. In Sec. 2, we describe the equations of the FLASH code and the physical configuration that were used in the simulations. In Sec. 3, we describe the key simulation results. In Sec. 4, we discuss the main results of simulations and draw conclusions.

2. Governing equations and simulation setup

We solve the following set of the ideal magnetohydrodynamic equations by using the FLASH code [14]:

$$\partial_t \rho + \nabla \cdot (\rho \mathbf{u}) = 0 \quad (1)$$

$$\partial_t (\rho \mathbf{u}) + \nabla \cdot \left[\rho \mathbf{u} \mathbf{u} - \frac{\mathbf{B} \mathbf{B}}{4\pi} + \mathbf{I} \left(p + \frac{B^2}{8\pi} \right) \right] = 0 \quad (2)$$

$$\partial_t \left[\rho \left(\frac{1}{2} u^2 + \epsilon \right) + \frac{B^2}{8\pi} \right] + \nabla \cdot \left[\rho \mathbf{u} \left(\frac{1}{2} u^2 + \epsilon + \frac{p}{\rho} \right) + \frac{c}{4\pi} \left(-\frac{\mathbf{u}}{c} \times \mathbf{B} + \mathbf{E}_B \right) \times \mathbf{B} \right] = 0 \quad (3)$$

$$\partial_t \mathbf{B} + \nabla \cdot (\mathbf{u} \mathbf{B} - \mathbf{B} \mathbf{u}) + c \nabla \times \mathbf{E}_B = 0 \quad (4)$$

$$\partial_t (\rho \epsilon_i) + \nabla \cdot (\rho \epsilon_i \mathbf{u}) + p_i \nabla \cdot \mathbf{u} = 0 \quad (5)$$

$$\partial_t (\rho \epsilon_e) + \nabla \cdot (\rho \epsilon_e \mathbf{u}) + p_e \nabla \cdot \mathbf{u} = 0 \quad (6)$$

where ρ is the mass density, \mathbf{u} the fluid velocity, \mathbf{B} the magnetic field, $p = p_e + p_i$ the fluid thermal pressure, $\epsilon = \epsilon_e + \epsilon_i$ the specific internal energy, $\mathbf{E}_B = -\nabla p_e / (en_e)$ the electric field inducing the BB mechanism under a baroclinic condition, and c the speed of light. The subscripts e and i refer to the electron species and ion species, respectively. For the equation of state, which connects the

*Corresponding authors

Email addresses: ryu201@postech.ac.kr (Chang-Mo Ryu), chulmin@gist.ac.kr (Chul Min Kim)

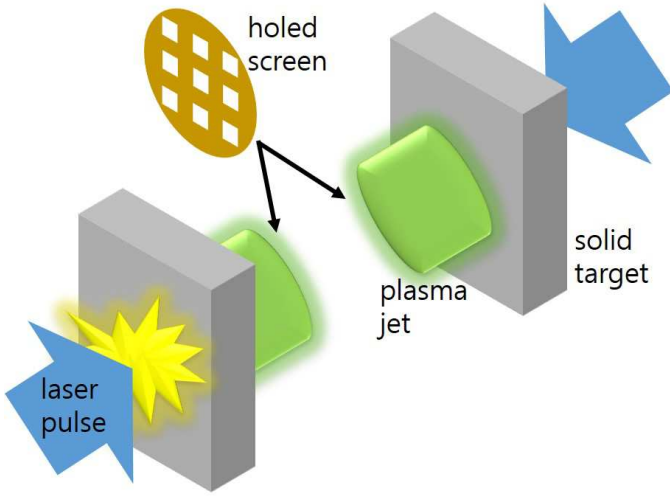


Figure 1: (Color online) Schematic diagram of the experimental configuration considered in our simulations. A plasma jet emerges from a laser-irradiated solid target, and after passing through a holed screen, the plasma becomes corrugated. By shifting one screen with respect to the other, the high density regions of a plasma jet collide with the low density regions of the counter-incoming jet, to maximize the KH instability.

internal energies to the pressures, the ideal gas law with a heat capacity ratio of $5/3$ is used for both species. We use the directionally unsplit staggered mesh solver that is a finite-volume high-order Godunov method with a constrained transport scheme for solving $\nabla \cdot \mathbf{B} = 0$ [15, 16]. The CFL number for the numerical stability is taken as 0.4. The number of grid cells used is $256 \times 128 \times 128$ for the volume of $0.8 \text{ cm} \times 0.4 \text{ cm} \times 0.4 \text{ cm}$.

We consider the colliding plasmas jets similar to the ones studied by Tzeferacos et al. [17, 13], which are produced from a laser-irradiated solid foil and pass through holed screens to give rise to a corrugated density distribution. The hole patterns of the two screens are shifted to each other so that the high-density parts of one jet collide with the low-density parts of the counter-incoming jets. We consider a similar situation as schematically shown in Fig. 1. We further simplify the situation as in Fig. 2, to clarify the dynamics in the colliding region. Plasma simulation parameters are chosen to be close to the ones used in Tzeferacos et al. [17] to make a direct comparison possible. The plasma in the left half plane ($x < 0.4 \text{ cm}$) collides with that in the right one. Each plasma has alternating low and high density channels of $\rho_L = 1.1 \times 10^{-6} \text{ g/cm}^3$ and $\rho_H = 4\rho_L = 4.4 \times 10^{-6} \text{ g/cm}^3$. Each plasma channel moves with a flow speed of $2.0 \times 10^7 \text{ cm/s}$.

The alternating density patterns of the left- and right-side plasma channels allows the KH instability to occur, when the plasma jets collide. The electron and ion temperatures are 50 eV and 100 eV, respectively. The sound speed in the high density regions is $4.7 \times 10^6 \text{ cm/s}$, and the corresponding Mach number is 4.3. In Tzeferacos et al.'s

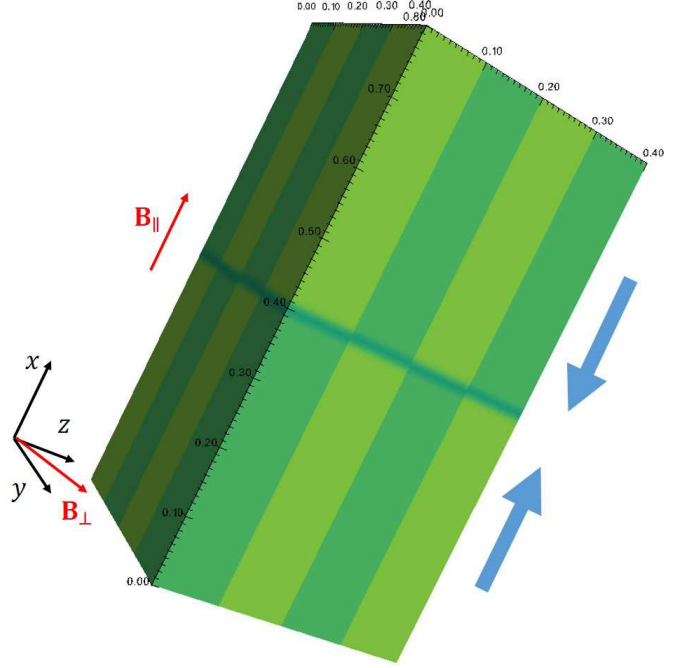


Figure 2: (Color online) 3D simulation geometry. The light green region and dark green region have densities of $\rho_H = 4.5 \times 10^{-6} \text{ g/cm}^3$ and $\rho_L = 1.1 \times 10^{-6} \text{ g/cm}^3$, respectively. Both regions have an initial flow speed of $|\mathbf{u}| = 2.0 \times 10^7 \text{ cm/s}$. The blue arrows denote the initial flow directions, and the red ones denote the directions of the perpendicular and parallel seed magnetic fields.

simulation [17], the magnetic field of about 4400 G is generated by the BB mechanism near the target region. This magnetic field is carried by the jet flows, which expand in time. Similarly, we have taken about 3000 G uniform magnetic field as a seed field in the parallel or perpendicular direction. We wish to examine whether there is any directional effect of the seed field. In actual experiments where the plasma jets are generated by irradiating a solid foil target with high-power lasers, the seed field is generated in the plasma by the BB process. In our simulation, we assume that a uniform magnetic field with a strength of 3000 G is embedded in the plasma before the collision starts to take place. The ratio of the kinetic energy to the magnetic energy is taken as 1410. For the plasma parameters chosen in our simulations, the resistivity and the viscosity are negligibly small. This justifies again the use of ideal MHD equations in (1)–(6).

3. Biermann battery effects on turbulent dynamo

When the plasma jets collide, plasma turbulence develops, and local density variation can increase rapidly. The geometry of the simulation setup is shown in Fig. 2. The direction of the seed magnetic field is shown as red arrows. The plasma jet colliding region is denoted by a blue layer in the middle.

In Fig. 3, mass density and magnetic energy density for the cases without the Biermann battery term are shown

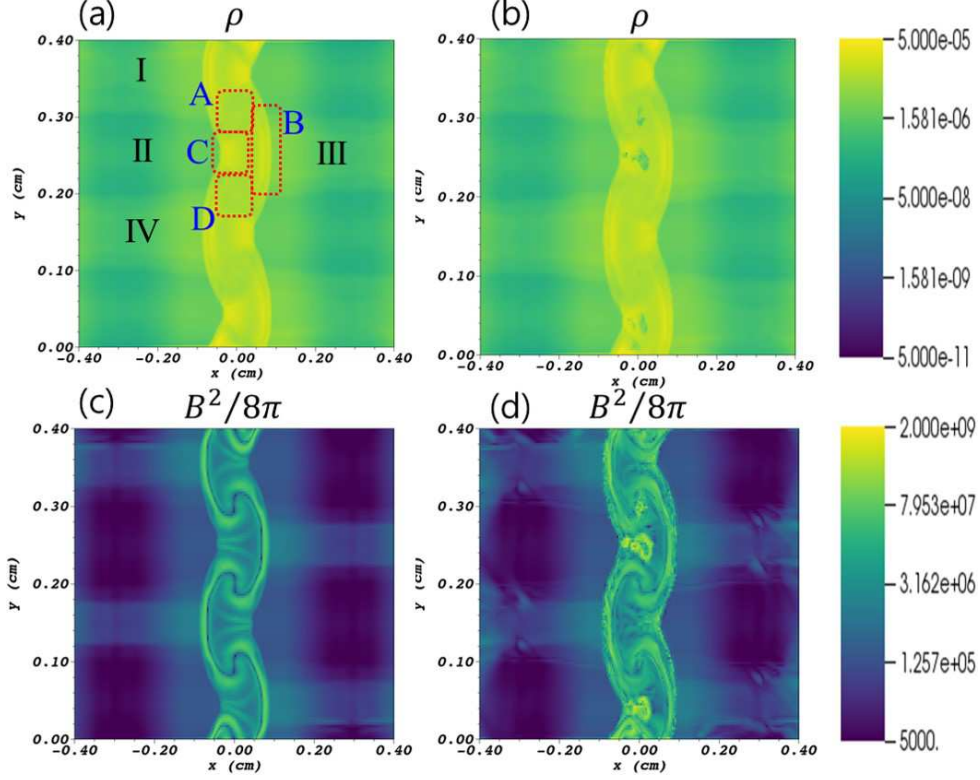


Figure 3: (Color online) Mass density and magnetic energy density on the plane at $z = 0.15$ cm at $t = 10$ ns. Mass density: (a) w/o BB and (b) w/ BB; magnetic energy density (c) w/o BB and (d) w/ BB. The initial magnetic field is perpendicular to the flow.

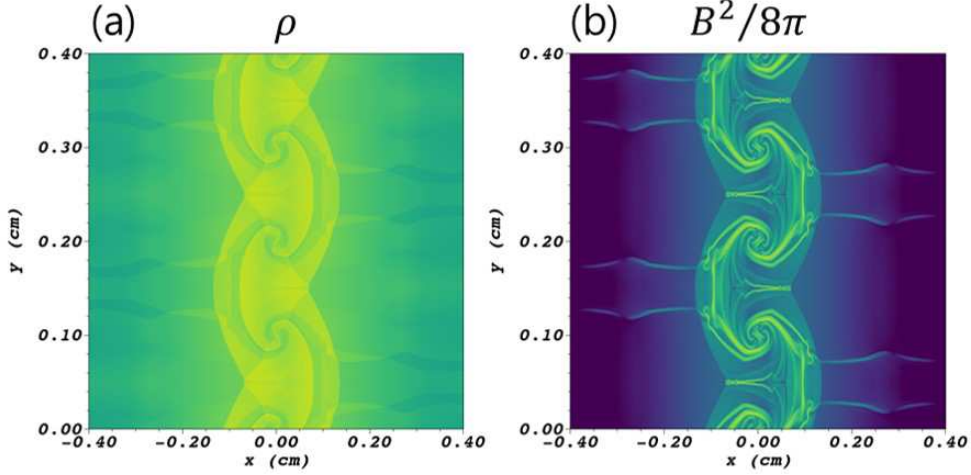


Figure 4: (Color online) 2D simulation results without BB at $t = 10$ ns: (a) mass density and (b) magnetic energy density. The initial magnetic field is perpendicular to the flow. The color scales are the same as in Fig. 3.

in (a) and (c) in comparison with those considering the Biermann battery term shown in (b) and (d), respectively. In the jet colliding region ($-0.1 \text{ cm} < x < 0.1 \text{ cm}$), the fluid is highly non-uniform; the large-scale inhomogeneity is marked by letters A, B, C, and D in Fig. 3(a). In region A, the KH instability grows due to the skew collision of high-density flows (I & III, and III & IV density column flows). The characteristic vortex structure is shown in the

magnetic energy density (Fig. 3(c)). The velocity vector field also shows a similar vortex structure. In region B, the fluid density is piled up toward the right half region due to the snow-ploughing action of the high density located in the left half region (II). Although this situation is similar to that found near the outer shells of supernova remnants [18], in our case, the Rayleigh–Taylor (RT) instability is not clearly observed. The mushroom structure seen in

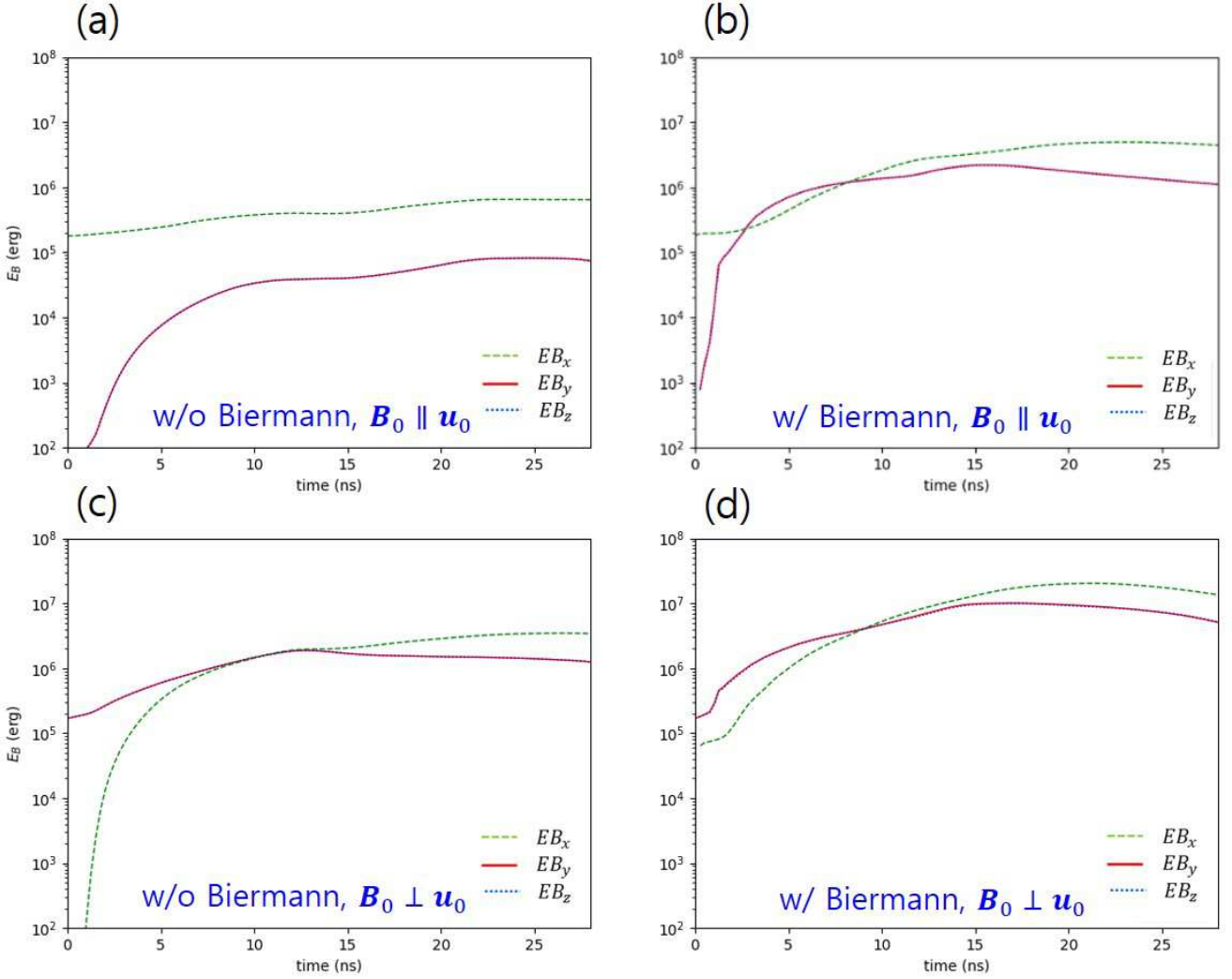


Figure 5: (Color online) Time evolution of magnetic energy: parallel B, (a) without Biermann battery (BB) and (b) with BB; perpendicular B, (c) without BB and (d) with BB. The curves for B_y and B_z overlap each other.

Fig. 3(c) is in fact an after effect of the KH instability (in regions A and D) and the density pile-up (in region B). We have also performed 2D simulations with a higher spatial resolution ($\Delta x_{2D} = \Delta x_{3D}/8$). As shown in Fig. 4, all the large-scale features in 3D simulations appear again, with finer details. The vortex structure also exists in the density plot. And the outer layer of the density profile has become thicker than in 3D simulations, exhibiting much finer structures.

In the case when the Biermann battery term is included, density holes can be shown at the center of the KH vortex and near the high density region, as shown in Fig. 3(b). The density hole seems to be associated with a pressure build up by a strong magnetic field, as can be noticed in Fig. 3(d). The small-scale structures induced by the development of turbulence seems to drastically enhance the Biermann Battery (BB) effect. This indicates that the BB can play an important role in turbulent dynamo.

Time evolution of magnetic energy is plotted in Fig. 5 for

the cases with and without the BB term, for the parallel and perpendicular magnetic fields, respectively. In this figure, B_y and B_z components are overlapped. The eddy turn over time can be estimated as $L/u = 0.1 \text{ cm}/(2.0 \times 10^7 \text{ cm/s}) = 5 \text{ ns}$, and at $t = 5 \text{ ns}$ the plasma fluid becomes already highly turbulent in agreement with simulations.

Figure 5 shows that the magnetic field amplification is greatly enhanced by the inclusion of the BB term. Furthermore, initially perpendicular seed fields bring a greater amplification than parallel ones. As shown in Fig. 5, strongest amplification is achieved when the seed field is perpendicular and the BB term is included. Such a configuration can be more relevant to the experiments than in the parallel case. In the actual experiment, the seed field is generated by the BB effect near the target, and it is perpendicular to the plasma flow because $\nabla n_e \times \nabla p_e$ is usually normal to the surface [19]. This seed field, then, is carried by the plasma flow. Therefore, in the experiment, we can expect a strong magnetic field amplification to occur, as indicated

in Fig. 5(d).

In obtaining Figs. 5(b) and (d), we reduced the Biermann term in Eq. (4) by a factor of 0.4 to avoid the Biermann catastrophe effects [20]. Without such modification, the magnetic field grows too rapidly in the simulation so that the calculation blows up in an early time. As the small scale develops by turbulence, the BB effect becomes stronger, making the numerical simulation more difficult. Even in the case of the reduced Biermann effect, its importance can be noticed.

4. Discussion and summary

Using the FLASH code, we have studied how the magnetic field is amplified in the colliding plasma jets. When the jet plasmas collide, they are compressed by collision, and the KH instability is excited from the early phase, and it develops into turbulence. Such turbulent fluid motion amplifies the magnetic field. The KH instability in a linear or nonlinear phase can contribute to the magnetic amplification. The magnetic field amplified by the KH turbulence can further be enhanced by the BB effects. The magnitude of field amplification depends on the direction of the initial seed magnetic field. For the initial field perpendicular to the plasma jet flow, the amplification by the BB effects is shown to be much stronger. To summarize, the BB can play an important role even in turbulent dynamo in laboratory and astrophysical plasmas. In Tzeferacos et al.'s studies on the turbulent dynamo [17, 13], the possibility of Biermann battery to contribute to the turbulent dynamo is ruled out. However, our results indicate that the Biermann battery coupled with the turbulent fluid motion might have contributed to their turbulence dynamo. Further study in this direction will be very worthwhile.

Acknowledgments

We acknowledge the fruitful discussions with P. Tzeferacos, A. Bott, and C. Graziani. This work was supported by IBS (Institute for Basic Science) under IBS-R012-D1, and also by GIST through the grant "Research on Advanced Optical Science and Technology." The software used in this work was developed in part by the DOE NNSA-ASC OASCR Flash Center at the University of Chicago.

References

- [1] H. Moffatt, Magnetic field generation in electrically conducting fluids, Cambridge, England, Cambridge University Press, 1978, 1978.
- [2] F. Krause, K.-H. Rädler, Mean-field magnetohydrodynamics and dynamo theory, Elsevier, 1980.
- [3] A. Brandenburg, K. Subramanian, Astrophysical magnetic fields and nonlinear dynamo theory, Phys. Rep. 417 (1-4) (2005) 1–209.
- [4] L. Biermann, On the origin of magnetic fields on stars and in interstellar space, Z. Naturforsch. A 5 (1950) 65–71.
- [5] R. M. Kulsrud, R. Cen, J. P. Ostriker, D. Ryu, The protogalactic origin for cosmic magnetic fields, The Astrophysical Journal 480 (2) (1997) 481.
- [6] E. S. Weibel, Spontaneously growing transverse waves in a plasma due to an anisotropic velocity distribution, Phys. Rev. Lett. 2 (3) (1959) 83.
- [7] M. V. Medvedev, A. Loeb, Generation of magnetic fields in the relativistic shock of gamma-ray burst sources, The Astrophysical Journal 526 (2) (1999) 697.
- [8] S. Fedotov, Non-normal and stochastic amplification of magnetic energy in the turbulent dynamo: Subcritical case, Physical Review E 68 (6) (2003) 067301.
- [9] M. V. Medvedev, R. A. Fonseca, L. O. Silva, M. Fiore, W. B. Mori, Generation of magnetic fields in cosmological shocks, J. Korean Astron. Soc. 37 (2004) 533–541.
- [10] K. Schoeffler, N. Loureiro, R. Fonseca, L. Silva, Magnetic-field generation and amplification in an expanding plasma, Phys. Rev. Lett. 112 (17) (2014) 175001.
- [11] N. Kugland, D. Ryutov, P. Chang, R. Drake, G. Fiksel, D. Froula, S. Glenzer, G. Gregori, M. Grosskopf, M. Koenig, et al., Self-organized electromagnetic field structures in laser-produced counter-streaming plasmas, Nat. Phys. 8 (11) (2012) 809.
- [12] C. Huntington, F. Fiuza, J. Ross, A. Zylstra, R. Drake, D. Froula, G. Gregori, N. Kugland, C. Kuranz, M. Levy, et al., Observation of magnetic field generation via the weibel instability in interpenetrating plasma flows, Nat. Phys. 11 (2) (2015) 173.
- [13] P. Tzeferacos, A. Rigby, A. Bott, A. Bell, R. Bingham, A. Casner, F. Cattaneo, E. Churazov, J. Emig, F. Fiuza, et al., Laboratory evidence of dynamo amplification of magnetic fields in a turbulent plasma, Nat. Commun. 9 (1) (2018) 591.
- [14] B. Fryxell, K. Olson, P. Ricker, F. Timmes, M. Zingale, D. Lamb, P. MacNeice, R. Rosner, J. Truran, H. Tufo, Flash: An adaptive mesh hydrodynamics code for modeling astrophysical thermonuclear flashes, The Astrophysical Journal Supplement Series 131 (1) (2000) 273.
- [15] D. Lee, A. E. Deane, An unsplit staggered mesh scheme for multidimensional magnetohydrodynamics, J. Comput. Phys. 228 (4) (2009) 952–975.
- [16] D. Lee, A solution accurate, efficient and stable unsplit staggered mesh scheme for three dimensional magnetohydrodynamics, J. Comput. Phys. 243 (2013) 269–292.
- [17] P. Tzeferacos, A. Rigby, A. Bott, A. Bell, R. Bingham, A. Casner, F. Cattaneo, E. Churazov, J. Emig, N. Flocke, et al., Numerical modeling of laser-driven experiments aiming to demonstrate magnetic field amplification via turbulent dynamo, Phys. Plasmas 24 (4) (2017) 041404.
- [18] S. Gull, The x-ray, optical and radio properties of young supernova remnants, Mon. Not. R. Astron. Soc. 171 (2) (1975) 263–278.
- [19] S. Eliezer, The interaction of high-power lasers with plasmas, CRC press, 2002.
- [20] C. Graziani, P. Tzeferacos, D. Lee, D. Q. Lamb, K. Weide, M. Fatenejad, J. Miller, The Biermann catastrophe in numerical magnetohydrodynamics, The Astrophysical Journal 802 (1) (2015) 43.